



Adaptive primary-multiple separation using 3D curvelet transform

Xiang Wu

CGG

Singapore

Xiang.Wu@cgg.com

Barry Hung

CGG

Singapore

Barry.Hung@cgg.com

SUMMARY

In this paper, we propose a method to enhance the separation of primaries and multiples by utilizing the ultra-sparseness property of the 3D curvelet transform. By extending our earlier work on the 2D method, our current 3D primary-multiple separation method takes into account the coherence between neighbouring gathers, and extends the Bayesian Probability Maximization (BPM) based separation mechanism into the 3D curvelet domain. The primaries and multiples are differentiated by utilizing the traces of neighbouring gathers in an additional dimension; this further promotes their separation compared to the 2D curvelet domain method. Moreover, this 3D curvelet domain separation method produces robust results regardless of the ordering of data as long as they are organized in a volumetric manner. Additionally, we have also introduced a 3D spatiotemporal constraint for handling the deviation from linearity or planarity of the seismic events. We demonstrate the improvement of the 3D curvelet domain primary-multiple separation method on synthetic and field data examples, by comparing the results with those produced by existing separation methods.

Key words: Primary-multiple Separation, 3D Curvelet, Ultra-sparseness, Least squares.

INTRODUCTION

Multiple attenuation is an important step in seismic processing. Residual multiple left over by incomplete attenuation will degrade the final image. In general, multiple attenuation involves two steps: the prediction/modelling of multiples and the separation of the multiples from the primaries. Considerable effort has been spent on the prediction of multiples in the last two decades. Surface-related Multiple Elimination (SRME) is used routinely in the industry to attenuate free-surface multiples; however, short-period and internal multiples are particularly problematic and have prompted significant research effort in recent years (Hargreaves, 2006; Wang, et al, 2012).

Apart from the advances in multiple prediction, an effective strategy for separating the multiples from the primaries is equally important. One of the most widely accepted separation strategies is the L2-norm based least-square separation method (LS) (Verschuur and Berkhout, 1997). It allows for a degree of inaccuracy in the multiple prediction, namely, the mismatch of traveltimes, amplitude and frequency spectrum between the predicted multiples and the recorded ones. However, a

compromise has to be made between the preservation of the primaries and the attenuation of the multiples, especially in places where the primary and multiple events cross one another or overlap. For this reason, curvelet-based separation methods have been attracting increasing attention in recent years. They have the advantage of minimizing the damage to the primary events which are separable from multiples in the curvelet domain (Herrmann et al., 2008). This separation stems from the curvelet transform decomposing energy based on its coherent dip, position, and frequency. Nevertheless, among various implementations of curvelet domain separation approaches, the non-adaptive implementations may encounter numerical divergence if the predicted multiples are very different from the multiples in the data; whereas, the adaptive implementations either only correct for limited misalignment between the predicted and actual multiples, or suffer from high computational cost due to the use of curvelet matching filters (Saab et al., 2007; Neelamani, et al., 2010). Very recently, a 2D high-fidelity adaptive curvelet domain separation method was proposed to remove the multiples while still preserving the masked primaries (Wu and Hung, 2013). Although the 3D curvelet transform has been used in denoising (Wang et al., 2013), it has not yet been, to the best of our knowledge, implemented for primary-multiple separation.

In this paper, we introduce a new approach to primary-multiple separation by utilizing the volumetric ultra-sparseness of seismic data in the 3D curvelet domain, and a separation mechanism that is applicable to sparsely represented data. In addition to relying on certain separation characteristics, i.e., dip, frequency and spatio-temporal position, within a 2D seismic gather, the method we propose places a strong importance on the coherence between neighbouring gathers so as to differentiate the multiples from the primaries. This further enhances the separability of primaries and multiples from the three dimensional perspective. In the following sections, we first demonstrate the ultra-sparseness of seismic data in the 3D curvelet domain. We then extend the adaptive separation mechanism to 3D and test its performance on synthetic datasets. Finally, we compare the results with those obtained using existing separation methods.

ULTRA-SPARSENESS OF 3D CURVELETS

The 3D curvelet transform is a multi-scale and multi-dimensional transform (Candès et al., 2006), and is written as:

$$C(j, \vec{k}, \vec{l}) = \int_{R^3} D(t, x, y) \varphi_{j, \vec{k}, \vec{l}}(t, x, y) dt dx dy$$

where $C(j, \vec{k}, \vec{l})$ is the curvelet coefficient indexed by its scale component j , solid-angle dip \vec{l} ((l_φ, l_θ)) in in-plane and out-of-

plane directions) and displacement \vec{k} ; $D(t, x, y)$ is the 3D seismic gather at time t and spatial locations x and y ; $\varphi_{j, \vec{k}, \vec{l}}(t, x, y)$ is the 3D curvelet basis. Both \vec{k} and \vec{l} increase in dyadic order in each dimension for every other j , hence the term “multi-scale”. In contrast to the time-space or frequency basis localized in either domain, a 3D curvelet is localized in both frequency and time-space domains, as defined by choice of the indices (Figure 1(b)). In addition to the linearity that 2D curvelets offer (Figure 1(a)), 3D curvelets also possess planarity due to the dimension expansion.

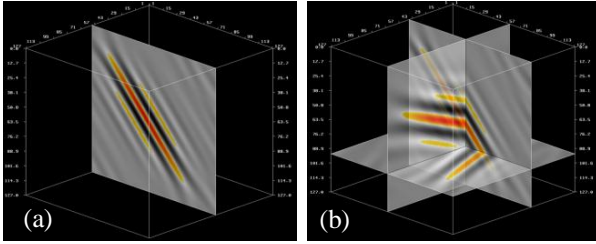


Figure 1. Illustration of (a): a 2D curvelet and (b): a 3D curvelet in 3D space.

Reflection events in seismic data follow the variation of the strata in the channel/shot domain and hyperbolic trajectories in the shot/channel domain; hence, for most conventionally ordered seismic data coherence exists in two spatial directions. It is due to either the nature of propagating waves or to the subsurface geology. These characteristics suit well the linear or planar nature of the 3D curvelets, which leads to the ultra-sparseness of seismic data in the 3D curvelet domain. We computed the 2D and 3D curvelet coefficients of the seismic section shown in Figure 2(a). Their distributions are shown in Figure 2(b). We can see a faster decay of the distribution of the 3D curvelet coefficients, which indicates greater level of sparsity for the 3D transform over the 2D transform. Both are expected to be sparser than time-space, Fourier or wavelet domain transforms (Candès *et al.*, 2006).

3D CURVELET DOMAIN PRIMARY-MULTIPLE SEPARATION

Apart from the least-square (LS) methods that minimize the total variation of the difference between seismic data and multiple models, there exists a way to exploit the sparseness introduced by the curvelet transform and to separate multiples from primaries. This is the separation mechanism based on Bayesian Probability Maximization (BPM) (Saab *et al.*, 2007) which was used in our previous work for 2D adaptive curvelet domain primary-multiple separation (Wu and Hung, 2013). If the prior probability distribution of coefficients of data and model is preset to a Gaussian form in BPM, the problem is reduced to a LS problem.

As discussed in above references, the enhancement of sparseness by the 3D curvelet transform guarantees the validation of the L1-norm in the BPM optimization problem. Herein, we extend the primary-multiple separation formalism by incorporating the 3D curvelet transform.

$$f(P_{c3}, M_{c3}) = \| |P_{c3}| \|_{1, w_1} + \| |M_{c3}| \|_{1, w_2} + \| |C_3^{-1} M_{c3} - f_{GA} * M' \|_2^2 + \eta \| |C_3^{-1} (P_{c3} + M_{c3}) - D \|_2^2$$

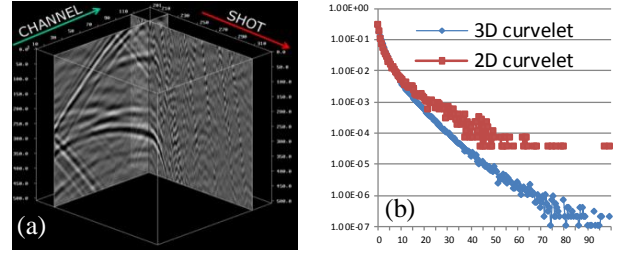


Figure 2. (a): The seismic section used to calculate the curvelet coefficients; (b): the distribution of 2D and 3D curvelet coefficients vs their values. The horizontal axis denotes the value of the curvelet coefficients relative to its maximum, in the unit of percentage; the vertical axis denotes the portion of the coefficients that is located around the value with a given interval tolerance.

where P_{c3} and M_{c3} denote the primaries and multiples in the 3D curvelet domain; D and M' are the data and the predicted multiple model in the time-space domain, respectively. C_3 denotes the forward 3D curvelet transform and C_3^{-1} its inverse. w_1 and w_2 are proportional to the 3D curvelet coefficients of the initial guess of model and data, and subscripts “1, w_* ” and “2” denote the element-wise weighted L1-norm, and L2-norm, respectively. η is the overall noise control parameter. f_{GA} is the global adaptation filter to precondition the raw multiple model by correcting its overall amplitude and traveltimes if these properties are deviated from that of the actual multiples. This method is referred to as 3D Adaptive Curvelet Domain Separation (ACDS-3D). An iterative soft-thresholding algorithm was used to solve this problem (Daubechies, *et al.*, 2004).

Moreover, a spatio-temporal constraint has been implemented into ACDS-3D. Such extension is mainly due to two reasons: 1): the seismic events might be strongly deviated from the linearity or planarity at a large scale and the sparseness of the coefficients may not be guaranteed. 2): the computational cost of the 3D curvelet transform is dramatically increased with the expansion of the operating size. For common seismic survey sizes, the method is only viable for research and testing purposes. Hence, a proper scale needs to be chosen in order to guarantee the sparseness of the seismic data in the 3D curvelet domain, and to cope with the spatiotemporal variation of the seismic data, e.g. amplitude and spectrum.

SYNTHETIC AND FIELD DATA EXAMPLES

We first assessed the performance of ACDS-3D on a simple example (Figure 3). For comparison, we show the results of the 2D adaptive curvelet domain separation (ACDS) method and the 3D least square (LS-3D) method. This example shows a typical case in which a horizontal multiple is fully overlapping with the primary reflection in the middle channel of Figure 3 (a1). ACDS works reasonably well in removing the multiple cutting through the primary. However, it fails to correctly separate the multiple in this example. This can be seen from the contamination of primary energy in the difference (Figure 3 (b2)) between the input (a1) and the result by ACDS (a2), in comparison with the true multiple (b1). LS-3D is a variant of the conventional planar least-square method, operating on a 3D volume. From column (3) (LS-3D), we found that there is a trade-off between preserving the primary and eliminating the multiple. In order to minimize the

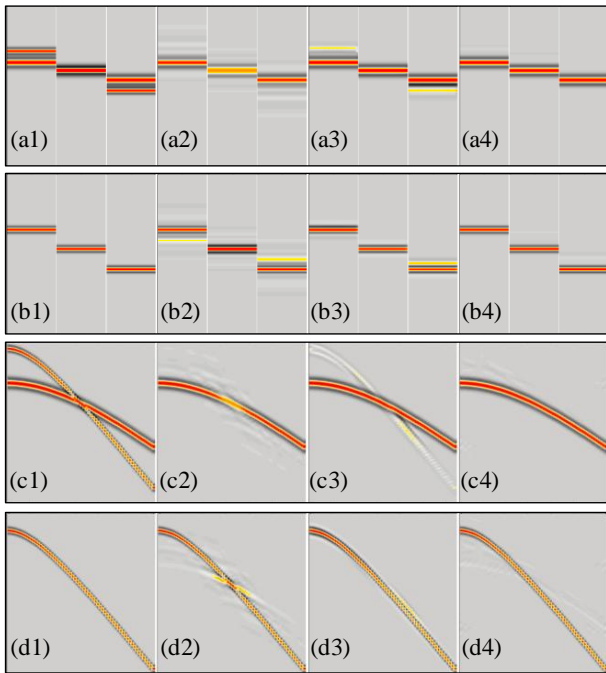


Figure 3. Synthetic Example 1: Rows (a) and (b) show the channel gathers (3 channels in 1 panel) of the primary-multiple separation results and differences between the input and results by (2) ACDS, (3) LS-3D and (4) ACDS-3D, respectively. (a1) is the input and (b1) is the multiple model. Rows (c) and (d) are the corresponding shot gathers of rows (a) and (b).

distortion of the primary, we displayed a conservative result produced by LS-3D; apparently, residual multiple energy is left behind in the result. In contrast, ACDS-3D makes minimal compromise between primary preservation and multiple removal. As shown in (a4) and (b4), the multiple is completely separated from the primary in both the shot and the channel domains. The advantage of the method is particularly noticeable in the middle channel where the multiple is removed despite the fact that it is thoroughly masked by the primary. This simple example has demonstrated the capability of ACDS-3D for primary-multiple separation. By making use of their characteristics (e.g., scales and dips) with an additional dimension in ACDS-3D, the separability of primaries and multiples is significantly enhanced and the continuity of the events in those dimensions is better preserved compared with the 2D method. Also, the incorporation of an ultra-sparseness and BPM-based algorithm in ACDS-3D outperforms the LS-3D method which is based on the minimization of the total variation.

We then tested the capability of ACDS-3D on surface multiple attenuation of a field data example. We still compare the results with the LS-3D and ACDS methods, as shown in Figure 4. In this example, SRME was applied to predict the surface-related multiples. The first order water-bottom related multiple and a strong primary event cut across one another with close dips in common channel gathers. They are severely overlapped in the middle channel gather, as shown in the right panel of Figure 4 (a1). In column (a), we found both 3D primary-multiple separation methods (LS-3D & ACDS-3D) are able to remove the multiple events in the aforementioned area of the middle channel gathers whereas the result by ACDS shows apparent remnants. Underneath the water

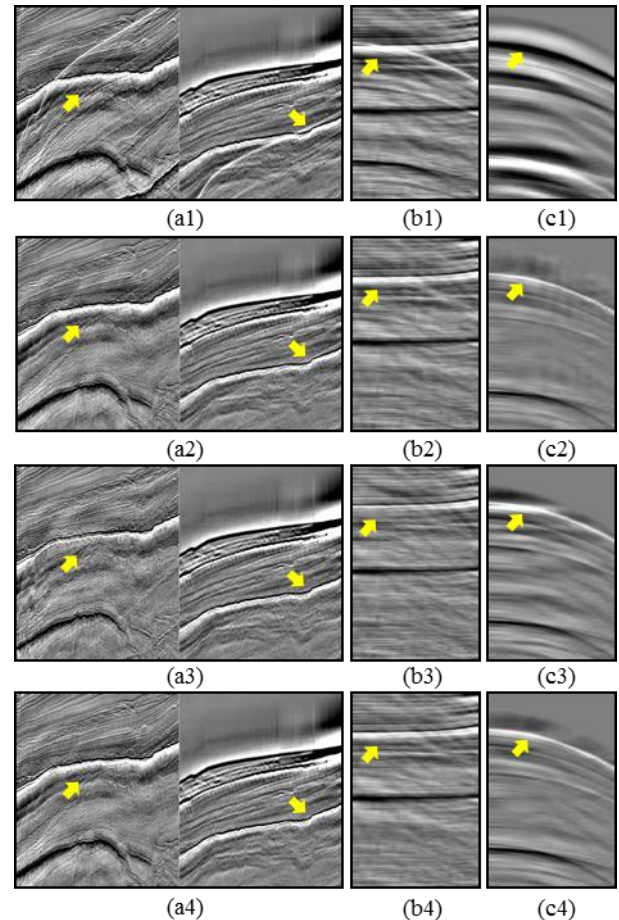


Figure 4. Field Data Example: Column (a): near (left panel) and middle (right panel) common channel gathers of (1) input, and the surface multiple attenuation results by (2) ACDS, (3) LS-3D and (4) ACDS-3D; Column (b): the corresponding CMP gathers; Column (c): (1) the CMP gather of the surface multiple model; the difference between input and the resulting CMP gathers by (2) ACDS, (3) LS-3D and (4) ACDS-3D.

bottom, primaries travel at higher speed (sound velocity in subsurface > 1500 m/s) than multiples do (sound velocity in water ≈ 1500 m/s). Such difference leads to difference of their moveout with respect to offsets. Hence, the level of overlap between the primary and the multiple changes or vanishes in the recording of different receivers, as can be seen in near and middle common channel gathers. Fortunately, this difference can be identified by 3D methods. Although LS-3D and ACDS-3D show comparable results in terms of multiple removal, severe contamination of primary energy is observed in the near channel gathers by LS-3D, as highlighted by the arrows in the left panel of Figure 4(a). In contrast, ACDS-3D preserves the primary well and removes the first order water-bottom related multiple at the meantime. This is because different degree of overlap between primaries and multiples from near to middle channels may require different parameterization of the matching filter, and this situation is difficult to be handled by a cuboidal filter performed on a volumetric window; ACDS-3D is free of filter parameters, and takes the volumetric coherence into account. Column (b) and (c) show the comparison of the separation methods in common mid-point (CMP) domain which is orthogonal to the domain we choose for separation. The selected CMP gather has a primary event overlaid by a strong multiple event in near

offsets. Similar phenomenon can be seen in that the primary in the near offsets is severely contaminated by LS-3D (Figure 4 (b3) & (c3)) but is well preserved by ACDS ((b2) & (c2)) and ACDS-3D ((b4) & (c4)). The reason for this is that the CMP domain is orthogonal to the domain of the separation process (common offset). The level of the overlap is then greatly reduced in that domain, which will not hinder the effectiveness of ACDS. Nevertheless, ACDS-3D still provides the superior result. Moreover, the vertical stripes in the shallow section of Figure 4 (c2) disappear in (c4) as ACDS-3D considers an extra dimension of coherence than ACDS.

CONCLUSIONS

To summarize, we have developed an adaptive primary-multiple separation method. It takes advantage of the ultra-sparseness inherited from the 3D curvelet transform and a Bayesian Probability Maximization mechanism. Synthetic and field data examples have demonstrated that our approach outperforms the conventional 3D least-squares method and the 2D adaptive curvelet domain separation method in terms of multiple removal and primary preservation. By taking into account the coherence of seismic data with an extra dimension, the separability between primaries and multiples is reinforced by the volumetric ultra-sparseness.

Primary-multiple separation in 2D often involves a choice of data processing domain in order to get better results. Nevertheless, our proposed 3D separation method produces robust result regardless of the choice of the favourite domain for separation. This comes from the intrinsic conformity between the 3D nature of this method and that of acquisition surveys (e.g. shot/channel configuration). Moreover, in order to validate the volumetric ultra-sparseness, we have introduced the spatiotemporal constraint by implementing local windowing.

ACKNOWLEDGMENTS

We acknowledge Apache Energy Ltd, INPEX Alpha Ltd and CGG management for granting permission to present this work. We would also like to thank Paul Bouloudas from Apache Energy Ltd for his valuable discussions and efforts in presenting the field data example, and Yi Xie, Guoyang Ye, Fong Cheen Loh, Yui Min Koh, and Todd Mojesky from CGG for their discussions and kind support.

REFERENCES

- Billette, F. J. and Brandsberg-Dahl, S., 2005, The 2004 BP velocity benchmark, EAGE Extended Abstracts, B035.
- Candès, E.J., Demanet L., Donoho, D.L., and Ying, L., 2006, Fast discrete curvelet transforms, SIAM Multiscale Model. Simul., 5, 861-899.
- Daubechies, I., Defrise, M., and De Mol, C., 2004, An iterative thresholding algorithm for linear inverse problems with a sparsity constraint, Comm. Pure Appl. Math., 57, 1413-1457.
- Hargreaves, N., 2006, Surface multiple attenuation in shallow water and the construction of primaries from multiples, SEG Expanded Abstracts, 2689–2693.
- Herrmann, F.J., Wang, D., and Verschuur, D.J., 2008, Adaptive curvelet-domain primary-multiple separation, Geophysics, 73, 17-21.
- Neelamani, R., Baumstein, A., and Ross, W. S., 2010, Adaptive subtraction using complex-valued curvelet transforms, Geophysics, 75, 51-60.
- Saab, R., Wang, D., Yılmaz, Ö., and Herrmann, F.J., 2007, Curvelet-based primary-multiple separation from a Bayesian perspective, SEG Expanded Abstract, 2510-2514.
- Verschuur, D. J., and Berkhout, A. J., 1997, Estimation of multiple scattering by iterative inversion, Part II: Practical aspects and examples, Geophysics, 62, 1596–1611.
- Wang, M., Hung, B., and Xin, K., 2012, Application of Inverse Scattering Series Method for Internal Multiple Attenuation: a case study, ASEG Extended Abstract, 1, 1-4.
- Wang, Y., Zhou, J., and Peng, J., 2013, 3D Seismic Denoise with 3D Curvelet Transform, SEG Extended Abstract, 4325-4329.
- Wu, X., and Hung, B., 2013, High-fidelity Adaptive Curvelet Domain Primary-Multiple Separation, 75th EAGE Conference & Exhibition incorporating SPE EUROPEC 2013, Tu-14-06.